Integrative Systems

Changes in GABAergic Transmission to and Intrinsic Excitability of Gonadotropin-Releasing Hormone (GnRH) Neurons during the Estrous Cycle in Mice

Caroline Adams,[1] Xi Chen,[1] and Suzanne M. Moenter[1,2,3]

Abstract

Gonadotropin-releasing hormone (GnRH) neurons form the final common central output pathway controlling fertility and are regulated by steroid feedback. In females, estradiol feedback action varies between negative and positive; negative feedback typically regulates episodic GnRH release whereas positive feedback initiates a surge of GnRH, and subsequently luteinizing hormone (LH) release ultimately triggering ovulation. During the estrous cycle, changes between estradiol negative and positive feedback occur with cycle stage and time of day, with positive feedback in the late afternoon of proestrus in nocturnal species. To test the hypotheses that synaptic and intrinsic properties of GnRH neurons are regulated by cycle stage and time of day, we performed whole-cell patch-clamp studies of GnRH neurons in brain slices from mice at two times considered negative feedback (diestrous PM and proestrous AM) and during positive feedback (proestrous PM). GABAergic transmission can excite GnRH neurons and was higher in cells from proestrous PM mice than cells from proestrous AM mice and approached traditional significance levels relative to cells from diestrous PM mice. Action potential response to current injection was also greater in cells from proestrous PM mice than the other two groups. Interestingly, the hormonal milieu of proestrous AM provided stronger negative feedback on both GnRH neuron excitability and GABAergic postsynaptic current (PSC) amplitude than diestrous PM. These observations demonstrate elements of both synaptic and intrinsic properties of GnRH neurons are regulated in a cycle-dependent manner and provide insight into the neurobiological mechanisms underlying cyclic changes in neuroendocrine function among states of estradiol negative and positive feedback.

Key words: action potential; estradiol; excitability; feedback; GABA; GnRH

Significance Statement

Infertility affects 15–20% of couples; failure to ovulate is a common cause. Understanding how the brain controls ovulation is critical for new developments in both infertility treatment and contraception. Gonadotropin-releasing hormone (GnRH) neurons are the final output pathway for central control of fertility and produce a signal that ultimately initiates ovulation in response to estradiol positive feedback. We studied how the reproductive cycle regulates both synaptic transmission to GnRH neurons and excitability of these cells. Both GABAergic transmission to GnRH neurons and GnRH neuron excitability are decreased during stages of the estrous cycle characterized by negative feedback by gonadal steroids, compared to the late afternoon of proestrus, when positive feedback and ovulation occur.

Introduction

Gonadotropin-releasing hormone (GnRH) neurons form the final hormonal output pathway through which the central nervous system controls reproduction. GnRH triggers the release of the anterior pituitary hormones, LH and follicle-stimulating hormone (Schally et al., 1971), which in turn promote sex steroid production and gametogenesis. In both sexes, gonadal steroid feedback controls GnRH release and pituitary response to GnRH (Levine and Ramirez, 1982; Karsch et al., 1987; Moenter et al., 1991). For most of the female reproductive cycle, the steroid estradiol suppresses total GnRH/LH release (negative feedback). However, at the end of the follicular phase (proestrus in rodents), sustained rising levels of estradiol switch from suppressing GnRH/LH release to inducing a surge of GnRH/LH release (positive feedback; Moenter et al., 1991; Czieselsky et al., 2016). The LH surge triggers ovulation.

In rodents, ovulation is tightly coupled to time-of-day (Everett and Sawyer, 1950; Sarkar et al., 1976). GnRH/LH surges typically begin ~1–2 h before lights out in nocturnal species with this positive feedback mode of hormone release being confined to the proestrous phase of the estrous cycle. Several paradigms for inducing positive feedback "surge" hormone release have been developed to study this phenomenon, with most involving ovariectomy and estrogen replacement (Norman et al., 1973; Legan and Karsch, 1975; Bronson and Vom Saal, 1979a; Bronson, 1981; Christian et al., 2005). Most studies of the biophysical properties of GnRH neurons during estradiol negative and positive feedback have made use of estrogen replacement surge-induction models.

To lay a basis for understanding how synaptic and intrinsic properties of GnRH neurons change between conditions of estradiol negative and positive feedback within the normal estrous cycle, we examined the rates of GABAergic fast synaptic transmission, the primary fast synaptic input to GnRH neurons, as well as GnRH neuron excitability, measured as action potential firing rate in response to current injection, and action potential prop-

erties. We compared proestrous PM, the time of positive feedback, with a low estradiol negative feedback stage (diestrous PM) and a high estradiol negative feedback stage (proestrous AM). We hypothesized that the transition among cycle stages induces changes in the intrinsic properties of GnRH neurons and GABAergic fast synaptic transmission to these cells.

Materials and Methods

All chemicals were purchased from Sigma-Aldrich, unless noted.

Animals

Transgenic mice expressing green fluorescent protein (GFP) under the control of the GnRH promoter (Tg(Gnrh1-EGFP)51Sumo MGI:6158457; GnRH-GFP mice) were used (Suter et al., 2000). Mice were housed on a 14/10 h light/dark cycle with lights off at 6 P.M. (eastern standard time). Teklad 2916 chow (Envigo) and water were available ad libitum. Estrous cycles of adult females aged 60–128 d were monitored by vaginal cytology to determine estrous cycle stage; mice were studied on diestrus or proestrus. Uterine mass was measured at the time of brain slice preparation to confirm cycle stage as it is directly proportional to circulating estradiol levels (Shim et al., 2000). Uterine mass was within the published range for diestrus ($n = 10$, 47.3 ± 2.7 mg) and proestrus (AM, $n = 8$, 131.3 ± 10.6 mg; PM, $n = 11$, 121.5 ± 2.7 mg; Silveira et al., 2017). Uterine mass was lower on diestrus (one-way ANOVA/Tukey's $F_{(2,26)} = 68.3$, $p < 0.0001$) than either time of day on proestrus and was not different between proestrous AM and PM ($p > 0.4$).

Brain slice preparation

All solutions were bubbled with 95% O_2/5% CO_2 throughout the experiments and for at least 15 min before exposure to tissue. Brain slices for AM recordings were prepared 8.5–9.5 h before lights out; slices for PM recordings were prepared 1.5–2.5 h before lights out. The time of PM slice preparation corresponds to 30 min before the onset "surge peak" window through the end of that window as defined in previous work (Christian and Moenter, 2007). The brain was rapidly removed and placed in ice-cold sucrose saline solution containing the following: 250 mM sucrose, 3.5 mM KCl, 26 mM NaHCO$_3$, 10 mM D-glucose, 1.25 mM Na$_2$HPO$_4$, 1.2 mM MgSO$_4$, and 3.8 mM MgCl$_2$, at pH 7.6 and 345 mOsm. Coronal (300 μm) slices were cut with a VT1200S Microtome (Leica Biosystems). Slices were incubated in a 1:1 mixture of sucrose saline and artificial CSF (ACSF) containing 135 mM NaCl, 3.5 mM KCl, 26 mM NaHCO$_3$, 10 mM D-glucose, 1.25 mM Na$_2$HPO$_4$, 1.2 mM MgSO$_4$, and 2.5 mM CaCl$_2$, at pH 7.4 and 305 mOsm, for 30 min at room temperature (~21–23°C). Slices were then transferred to 100% ACSF at room temperature for 0.5–5 h before recording.

Data acquisition

During recording, slices containing the preoptic area and anterior hypothalamus, which contain the majority of GnRH neuron somata, were placed into a chamber continuously perfused with ACSF at a rate of 2 ml/min with

oxygenated ACSF heated to 29.5–31.5°C with an inline-heating unit (Warner Instruments). GFP-positive cells were visualized with a combination of infrared differential interference contrast and fluorescence microscopy on an Olympus BX50WI or BX51WI microscope. Borosilicate glass capillaries (1.65-mm OD × 1.12-mm ID; World Precision Instruments, Inc.) were pulled by using a Flaming/Brown P-97 unit (Sutter Instrument Company) to make recording pipettes. Pipettes measured 2–4.5 MΩ when filled with: 125 mM K gluconate, 20 mM KCl, 10 mM HEPES, 5 mM EGTA, 0.1 mM $CaCl_2$, 4 mM MgATP, and 0.4 mM NaGTP; 300 mOsm, pH 7.2 with NaOH for current-clamp recordings or when filled with: 140 mM KCl, 10 mM HEPES, 5 mM EGTA, 0.1 mM $CaCl_2$, 4 mM MgATP, and 0.4 mM NaGTP; 300 mOsm, pH 7.2 with NaOH for recording GABAergic PSCs. Pipettes were wrapped with Parafilm (Bemis) to reduce capacitive transients; remaining transients were electronically cancelled. Pipettes were placed in contact with a GFP-positive neuron using an MP-285 micromanipulator (Sutter Instrument Company). All potentials reported were corrected online for liquid junction potential of -14.2 mV for the K gluconate pipette solution and 4.9 mV for the 140 mM KCl pipette solution. (Barry, 1994). Recordings were made with an EPC-10 dual patch-clamp amplifier (HEKA Elektronik) and Patchmaster software (HEKA Elektronik). Experiments were analyzed offline using custom software (DeFazio and Moenter, 2002; DeFazio et al., 2014) written in IgorPro (Wavemetrics).

Experimental design

Comparisons of the properties of GABAergic transmission to GnRH neurons and the intrinsic firing properties of GnRH neurons in response to current injection were made among cells in brain slices from diestrous PM, proestrous AM, and proestrous PM mice.

Whole-cell patch-clamp

After achieving a >1 GΩ seal and the whole-cell configuration, membrane potential was held at -60 mV between protocols. Series resistance (R_s), input resistance (R_{in}), and holding current (I_{hold}) were measured every 2–3 min using a 5-mV hyperpolarizing step from -60 mV (mean of 20 repeats, 20-ms duration, sampled at 100 kHz and filtered at 10 kHz). Only recordings with a R_{in} of >500 MΩ, I_{hold} of $-50 - 20$ pA, stable R_s of <20 MΩ, and a stable Cm between 8.5 and 23 pF were used for analysis.

Spontaneous GABAergic postsynaptic currents (sPSCs) were measured in voltage-clamp at a holding potential of -70 mV. Current was sampled at 10 kHz and filtered at 10 kHz. ACSF contained 20 μM D-APV (Tocris), and 20 μM CNQX to block ionotropic glutamate receptors. At least two 120-s recordings were made for each cell for determining sPSC frequency. Mean ± SEM recording time was 591 ± 107 s/cell for diestrous PM ($n = 11$, range 240–1200 s), 457 ± 46 s/cell for proestrous AM ($n = 9$, range 240–600 s), and 536 ± 56 s/cell during proestrus PM ($n = 16$, range 244–1010 s). A total of 1351, 446, and 7929 sPSC events were recorded during diestrous PM, proestrous AM, and proestrous PM, respectively.

To measure activity-independent miniature PSCs (mP-SCs), at least two to three 120-s recordings were made before and during bath application of 1 μM tetrodotoxin (TTX, Tocris) in a separate set of cells from the diestrous PM and proestrous PM groups.

GnRH neuron excitability was assessed in current-clamp recordings. Direct current was adjusted to keep cells within 2 mV of -69 mV. Membrane potential was sampled at 20 kHz and filtered at 7.3 kHz. Bridge balance (95%) was used for most cells; for a few cells in diestrous PM and proestrous PM groups, bridge balance was not used but results were similar. ACSF contained 100 μM picrotoxin, 20 μM D-APV, and 20 μM CNQX to block ionotropic GABA and glutamate receptors. Cells were injected with current from 0 to 30 pA (500 ms, 2-pA steps). This protocol was repeated two to three times per cell and the number of action potentials at each step was averaged. The first spike fired was used to determine the following action potential characteristics: latency from start of the current injection to first spike, firing threshold (membrane potential when the first derivative of the voltage trace exceeds 1 V/s), peak amplitude relative to threshold, full width at half-maximum (FWHM), rate-of-rise, and time and amplitude of after-hyperpolarization potential (AHP; both relative to threshold).

Statistical analyses

Data were analyzed using Prism 7 (GraphPad) or SPSS (IBM) and are reported as the mean ± SEM. The number of cells per group is indicated by n. No more than two cells were used per animal with at least four animals tested per group. One cell from the diestrous PM GABA transmission group was identified as an outlier by ROUT (robust regression and outlier removal) with a strict Q coefficient of 0.01 and was excluded from all data sets. Data distribution was determined using a Shapiro–Wilk test for normality. Amplitudes of sPSC were binned at 5-pA intervals and histograms constructed of the mean on a per cell basis. Interevent intervals were binned at 0.1 s and plotted as a cumulative probability; events in cells from the proestrous AM group were sufficiently infrequent that the histogram of these data was not informative. Recordings with zero events were excluded from interevent interval analysis; values reported are thus an underestimate of interevent interval as the maximum that could be considered was two minutes. ANOVA analyses did not assume equal subgroup sizes. Tests are specified in the results and legends; $p < 0.05$ was accepted as significant.

Results

GABAergic transmission to GnRH neurons is increased during proestrus

In the daily surge model (Christian et al, 2005), GABAergic transmission is decreased during negative feedback and increased during positive feedback relative to OVX controls (Christian and Moenter, 2007). To examine whether GABA transmission to GnRH neurons is modulated between phases of the estrous cycle during which physiologic negative versus positive feedback are ob-

served, GABAergic sPSCs were recorded from GnRH neurons in brain slices obtained from diestrous PM, proestrous AM (both negative feedback), or proestrous PM (positive feedback) mice. Representative recordings are shown in Figure 1A, and recording parameters in Table 1. Frequency of GABAergic sPSCs was increased during proestrous PM relative to proestrous AM and approached traditional significance values versus diestrous PM (Fig. 1B; diestrous PM $n = 11$, proestrous AM $n = 9$, proestrous PM $n = 16$, Kruskal–Wallis/Dunn's, $p = 0.063$ proestrous PM vs diestrous PM, $p < 0.001$ proestrous AM vs proestrous PM). Interestingly, although mean frequency of GABA transmission from cells recorded on diestrous PM was not different from proestrous AM, the cumulative probability distribution of sPSC interevent interval averaged by cell differed significantly among all groups. Specifically, the distribution was shifted toward shorter intervals on proestrous PM and longer intervals for proestrous AM, both being different from the intermediate distribution for diestrous PM events and from one another (Fig. 1C; Kruskal–Wallis/Dunn's, proestrous AM vs both proestrous PM and diestrous PM, $p < 0.0001$; diestrous PM vs proestrous PM, $p < 0.0001$). Cumulative distributions can be skewed by one or two high frequency cells; in these data sets, the median and interquartile range followed the same pattern as the mean (diestrous PM 0.18 Hz [IQR 0.10–0.32], proestrous AM 0.02 Hz [0.001–0.16], proestrous PM 0.57 Hz [0.30–1.91]).

Amplitude of sPSCs was also markedly suppressed in cells from proestrous AM mice (Fig. 1D,E; one-way ANOVA/Tukey, proestrous AM $p < 0.05$ vs diestrous PM, proestrous AM $p < 0.005$ vs proestrous PM). Consistent with this observation, the peak of the amplitude histogram was significantly left-shifted for proestrous AM cells versus diestrous PM and proestrous PM cells (Fig. 1F; Kruskal–Wallis/Dunn's, $p < 0.001$). No difference was observed in decay time between 90% and 10% of the maximum current amplitude (Fig. 1G; ANOVA, $p > 0.2$).

GABAergic transmission is primarily activity independent and does not change between diestrus and proestrus

Increased GABAergic PSC frequency during proestrus may be due to an increase in presynaptic activity and/or synaptic release sites on GnRH neurons. To differentiate between these mechanisms, PSC frequency and amplitude were recorded before and during treatment with the voltage-gated sodium channel blocker TTX (Fig. 2A). TTX treatment isolates activity-independent neurotransmission, which is proportionate to the number of functional synaptic connections as well as to release probability at individual release sites (Auger and Marty, 2000; Kaeser and Regehr, 2014). Because the frequency of overall GABAergic transmission was very low in cells recorded on proestrous AM, they were excluded from this analysis. Neither PSC frequency nor amplitude (Fig. 2B–D; two-way repeated-measures ANOVA/Bonferroni) were altered during TTX treatment ($n = 6$ cells diestrous PM, $n = 5$ cells proestrous PM). An increase in PSC decay time during TTX was detected by ANOVA, but post hoc tests did not

detect differences within cycle stage (Fig. 2E; two-way repeated-measures ANOVA, TTX: $F_{(1,9)} = 6.4$, Bonferroni: $p = 0.22$ for both groups). Collectively these data indicate that most synaptic transmission observed in the slice is activity independent and that this does not change between the cycle stages examined.

GnRH neuron excitability is increased during positive feedback

To investigate whether GnRH neuron excitability is also modulated during the estrous cycle, we measured GnRH neuron response to depolarizing steady-state current injections (0–30 pA, 2-pA steps, 500 ms). Figure 3A shows representative responses to +12 and +24 pA injections. The rheobase current (the minimum current required to initiate spikes) was lowest on proestous PM during positive feedback and highest on proestrous AM (Fig. 3C; diestrous PM $n = 9$, proestrous AM $n = 7$, proestrous PM $n = 9$, one-way ANOVA/Tukey, $p < 0.05$ diestrous PM vs both proestrous AM and proestrous PM, $p < 0.0001$ proestrous AM vs proestrous PM). Once firing was initiated, GnRH neurons from proestrous PM mice fired more spikes. Specifically, at current steps from 12 to 30 pA, cells recorded on proestrous PM fired more spikes than cells from either diestrous PM mice or proestrous AM mice (Fig. 3B; two-way repeated-measures ANOVA/Fisher's LSD, $p < 0.05$). Differences were also observed between the two negative feedback stages examined; at current steps ≥ 20 pA, cells from proestrous AM mice fired fewer spikes than cells from diestrous PM mice. Rin was lower in cells recorded on proestrous AM; this could contribute to fewer spikes being fired in this group (Table 1).

A number of action potential properties were also altered among the cycle stages examined, including action potential threshold being hyperpolarized on proestrous AM versus diestrous PM (Fig. 3E; ANOVA/Tukey, $p < 0.01$) and rate-of-rise being lower on proestrous AM than proestrous PM (Fig. 3H; Kruskal–Wallis/Dunn's, $p < 0.05$). FWHM was greater on proestrous AM than both other groups (Fig. 3G; ANOVA/Tukey, $p < 0.0001$). Afterhyperpolarization time was reduced on proestrous PM compared to diestrous PM (Fig. 3J; Kruskal–Wallis/Dunn's, $p < 0.05$). No cycle-dependent changes were observed in time to first spike (spike latency; Fig. 3D; ANOVA $p = 0.0792$), AP spike amplitude (Fig. 3F; ANOVA, $p > 0.5$), or AHP amplitude (Fig. 3I; ANOVA, $p > 0.5$).

Discussion

The female reproductive cycle is characterized by one of the rare examples of positive feedback in physiology, specifically the induction of a surge mode of GnRH and LH release at the end of the follicular phase (proestrous PM in nocturnal rodents). This is largely attributed to exposure to high sustained levels of estradiol from the mature Graafian follicle(s) (Docke and Dorner, 1965). Here, we show that GABAergic transmission to GnRH neurons and GnRH neuron excitability are both increased during positive feedback (proestrous PM) relative to two different representations of negative feedback, diestrous
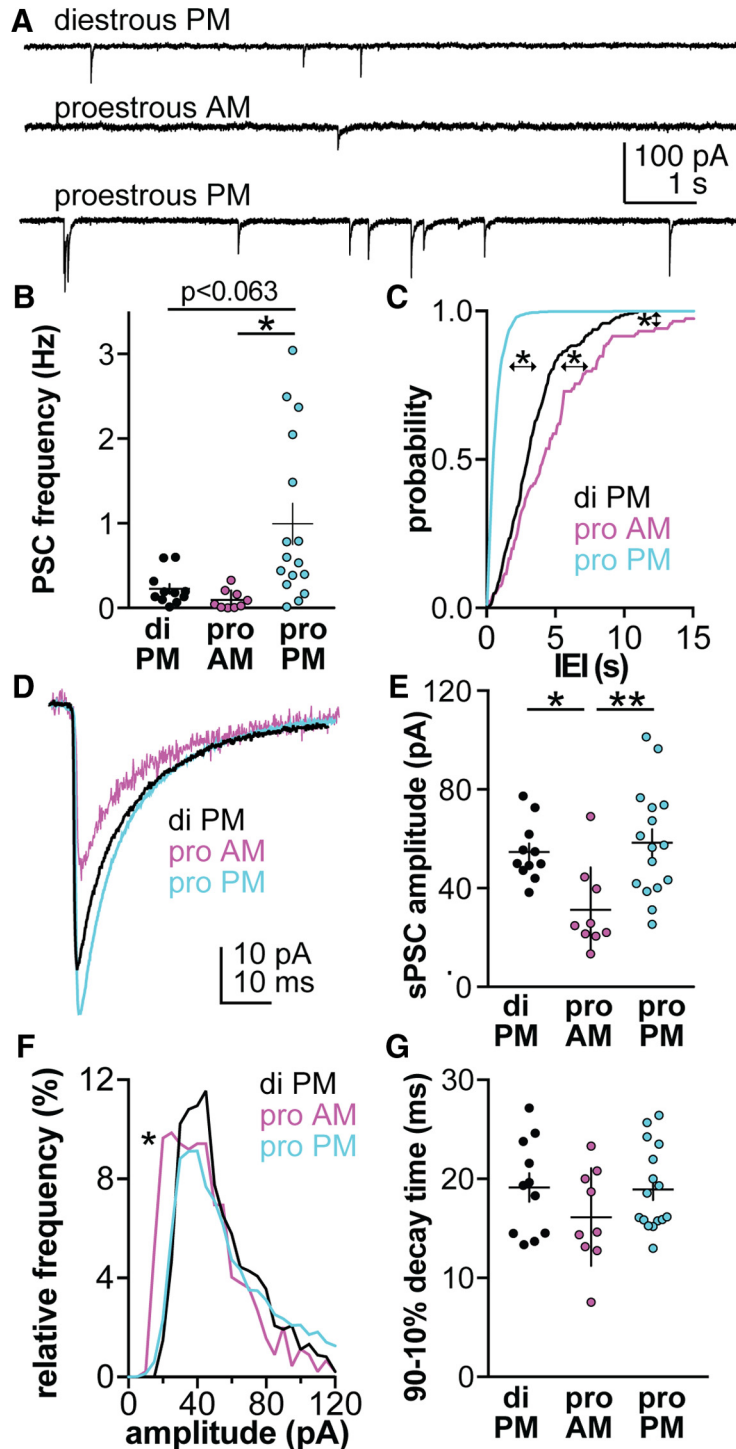
Figure 1. GABAergic sPSC frequency is highest on proestrous PM. **A**, Representative sPSC recording from a neuron in each group. **B**, Individual values and mean ± SEM of spontaneous GABAergic PSC frequency for cells recorded on diestrous (di) PM, proestrous (pro) AM and pro PM (Kruskal–Wallis, KW = 14.4, *$p < 0.05$ Dunn's). **C**, Mean by-cell cumulative probability distribution of interevent interval (IEI) for each group (Kruskal–Wallis, KW = 191, *$p < 0.0001$, Dunn's). **D**, By-cell average of all sPSC from all cells in each group. **E**, Individual values and mean ± SEM of sPSC amplitude (ANOVA $F_{(2,33)} = 6.69$, *$p < 0.05$, **$p < 0.005$ Tukey). **F**, Histogram of mean by-cell sPSC amplitude distribution (Kruskal–Wallis, KW = 23.9, proestrous AM vs both diestrous PM and proestrous PM, *$p < 0.001$, Dunn's). **G**, Individual values and mean ± SEM of sPSC time decay time between 90% and 10% of the maximum event amplitude (ANOVA $F_{(2,33)} = 1.34$).

Table 1 . Whole-cell recording properties for Figures 1–3

Mean ± SEM of GnRH whole-cell passive properties from Figure 1			
	Diestrous PM	Proestrus AM	Proestrus PM
R_{in} (MΩ)	929 ± 42	1336 ± 160*	1034 ± 63
Capacitance (pF)	14.7 ± 0.7	13.0 ± 0.8	14.5 ± 0.7
R_s (MΩ)	13.2 ± 0.6	13.5 ± 1.0	14.6 ± 0.7
I_{hold} (pA)	-13.6 ± 4.2	-0.15 ± 4.7#	-17.4 ± 2.8

*$p < 0.05$ vs diestrous PM; #$p < 0.01$ vs proestrous PM, Tukey's

ANOVA parameters for comparison of GnRH passive properties (Fig. 1)

R_{in} (MΩ)	$F_{(2,33)} = 4.84$
Capacitance (pF)	$F_{(2,33)} = 1.32$
R_s (MΩ)	$F_{(2,33)} = 0.951$
I_{hold} (pA)	$F_{(2,33)} = 5.38$

Mean ± SEM of GnRH whole-cell passive properties from Figure 2

	Diestrous PM	Proestrus PM
R_{in} (MΩ)		
Before TTX	1053 ± 88	1113 ± 145
During TTX	846 ± 83	775 ± 91
Capacitance (pF)		
Before TTX	15.8 ± 0.8	13.2 ± 0.9
During TTX	15.0 ± 0.8	13.8 ± 1.0
R_s (MΩ)		
Before TTX	12.1 ± 0.9	12.3 ± 0.6
During TTX	13.3 ± 1.5	14.7 ± 0.8
I_{hold} (pA)		
Before TTX	-16.4 ± 3.5	-19.4 ± 2.6
During TTX	-25.1 ± 6.3	-28.5 ± 3.8

Two-way repeated measures ANOVA for comparison of GnRH passive properties among groups (Fig. 2)

	Group	TTX	Group × TTX
R_{in} (MΩ)	$F_{(1,9)} = 0.001$	$F_{(1,9)} = 36.0$***	$F_{(1,9)} = 2.1$
Capacitance (pF)	$F_{(1,9)} = 2.5$	$F_{(1,9)} = 0.1$	$F_{(1,9)} = 6.9$*
R_s (MΩ)	$F_{(1,9)} = 0.4$	$F_{(1,9)} = 6.0$*	$F_{(1,9)} = 0.7$
I_{hold} (pA)	$F_{(1,9)} = 0.3$	$F_{(1,9)} = 14.1$**	$F_{(1,9)} = 0.01$

Mean ± SEM of GnRH whole-cell passive properties from Figure 3

	Diestrous PM	Proestrus AM	Proestrus PM
R_{in} (MΩ)	1125 ± 150	667 ± 43*	1361 ± 144
Capacitance (pF)	13.7 ± 0.7	13.8 ± 0.7	12.5 ± 0.8
R_s (MΩ)	13.5 ± 0.9	11.9 ± 0.9	13.5 ± 1.4
I_{hold} (pA)	-0.7 ± 5.2	-2.8 ± 6.3	-10.1 ± 4.4

*$p < 0.05$ vs diestrous PM, Tukey's

ANOVA parameters for comparison of GnRH passive properties (Fig. 3)

R_{in} (MΩ)	$F_{(2,22)} = 6.65$
Capacitance (pF)	$F_{(2,22)} = 1.02$
R_s (MΩ)	$F_{(2,22)} = 0.62$
I_{hold} (pA)	KW = 3.36

switch to positive feedback (Evans et al., 1997). The levels of estradiol achieved in the daily surge model (Christian et al., 2005) are in the physiologic range, but are persistently, rather than cyclically, elevated, and the result is daily changes from negative to positive feedback. Because estradiol level is similar during negative and positive feedback, it is not an estradiol rise that triggers the change between states in this model. This differs from the estrous cycle in which an estradiol rise is viewed as the trigger for the transition. The question is thus raised of whether or not underlying mechanistic differences observed between feedback states in the daily surge model are the same as those during the cycle. The similar increase in GnRH neuron excitability and GABA transmission observed during positive feedback in the present work in cycling mice to published observations in the OVX+E daily surge model indicates at least some of the neurobiological mechanisms underlying the feedback switch are similar between these models. Consistent with these observations, GnRH neuron firing rate has also been shown to be similar during positive feedback whether induced by OVX+E or occurring spontaneously on the afternoon of proestrus (Silveira et al., 2017).

Of interest, the two negative feedback stages studied also diverged from one another with regard to some of the parameters examined. Specifically, cells studied on the morning of proestrus were less excitable and had smaller amplitude GABAergic PSCs than cells on the afternoon of diestrus. Both estradiol and progesterone change with cycle stage and either or both may underlie these observations. Progesterone typically provides negative feedback on GnRH release and firing rate (Moenter et al., 1991; Barrell et al., 1992; Pielecka et al., 2006). In the present studies we have no measure of progesterone, but it is likely that the influence of this steroid would be greater on diestrous PM than proestrous AM. Based on uterine mass, we can surmise that estradiol levels were higher on the morning of proestrus than on the afternoon of diestrus. The reduced excitability and transmission observed on proestrous AM relative to diestrous PM may thus be a consequence of the increase in estradiol inducing a biphasic feedback response, with negative feedback preceding positive feedback. In this regard, administration of a surge-inducing dose of estradiol to ovariectomized females initially suppresses and then increases GnRH release (Moenter et al., 1990). Similar observations have been made during reproductive cycles of sheep and women, in which the amplitude of LH pulses is reduced as the follicular phase proceeds, coincident with rising estradiol levels. In the present study, some action potential parameters appeared to change sooner on exposure to the cyclical rise in estradiol (e.g., the hyperpolarization of threshold) than others (e.g., increased rate of rise). Still others exhibited biphasic changes on exposure to the estradiol rise (e.g., rheobase and FWHM). Together, these observations suggest both that estradiol action during the mouse cycle is biphasic and that the negative feedback signal provided by high estradiol before transition to positive feedback on proestrus is stronger than that produced by the hormonal milieu on diestrus. This indicates the

PM and proestrous AM, which, interestingly, also diverged from one another in some aspects.

The present observations support and extend work in an OVX+E mouse model in which the switch from estradiol negative to positive feedback occurs solely on a time-of-day basis, referred to as the daily surge model (Christian et al., 2005). Estradiol must be elevated near peak follicular phase levels for several hours to initiate the
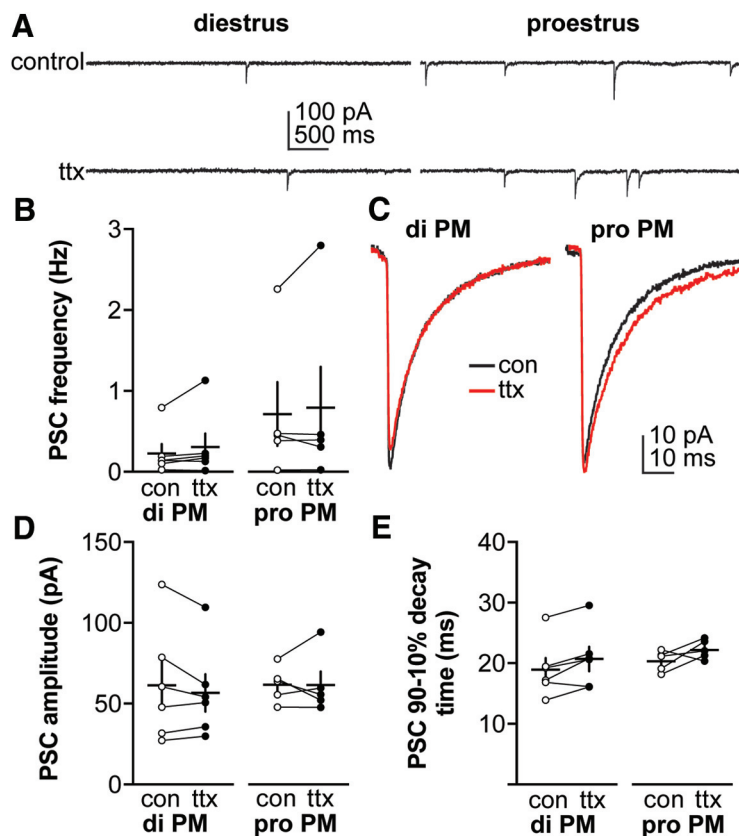
Figure 2. Blocking action potentials does not affect GABAergic PSC frequency or amplitude in diestrous or proestrous mice. *A*, Representative recordings from a representative neuron in each group before (control or con, top) and during (bottom) TTX treatment (from $n = 6$ cells diestrous PM, $n = 5$ cells proestrous PM). *B*, Individual values and mean $\pm$ SEM of GABAergic PSC frequency. *C*, Average of all PSC traces for control or ttx periods from all cells in each group. *D, E*, Individual values and mean $\pm$ SEM for: (*D*) PSC amplitude, (*E*) decay time between 90% and 10% of the maximum current amplitude. No statistical differences were detected using two-way repeated-measures ANOVA/Bonferroni test (*B*, cycle stage: $F_{(1,9)} = 1.3$; TTX: $F_{(1,9)} = 1.6$; cycle stage $\times$ TTX: $F_{(1,9)} = 0.0$; *D*, cycle stage: $F_{(1,9)} = 0.3$; TTX: $F_{(1,9)} = 0.6$; cycle stage $\times$ TTX: $F_{(1,9)} = 0.5$; *E*, cycle stage: $F_{(1,9)} = 0.5$; TTX: $F_{(1,9)} = 6.4$ ($p = 0.01$); cycle stage $\times$ TTX: $F_{(1,9)} = 0.9$).

strong negative feedback observed in the AM of the OVX+E daily surge model may more closely resemble proestrous AM than diestrous PM.

The shift from negative to positive feedback from proestrous AM to proestrous PM is consistent with the biphasic effects of estradiol, but may be augmented by other steroid changes. In addition to its role during negative feedback, progesterone can also amplify the LH surge in rats and mice (Bronson and Vom Saal, 1979b). Studies have also identified central changes induced by progesterone and ligand-independent actions of the progesterone receptor as important for positive feedback (Chappell et al., 1999; Chappell and Levine, 2000; Micevych and Sinchak, 2011). The amplitude of the proestrous LH surge in mice is greater than the estradiol-induced surge, attributable at least in part to augmented pituitary response to GnRH on proestrus (Silveira et al., 2017). In women, progesterone administration during the late follicular phase augments LH pulse amplitude, which could be attributable to increased amplitude GnRH release and/or increased responsiveness to endogenous GnRH, but does not alter pulse frequency, which would require central action (Hutchens et al., 2016). Of interest

to the site of progesterone action, the excitability parameters observed in the present study on the afternoon of proestrus, when both progesterone and estradiol from the ovary were present before brain slice preparation, are remarkably similar to those during positive feedback in OVX+E daily surge mice (Adams et al., 2018), which have been exposed to only circulating estradiol for at least 2 d. These observations may indicate boosting effects of progestins on LH surge amplitude occur independent of GnRH neurons at the level of the anterior pituitary; such action could be directly on the pituitary and/or indirectly via alterations of other neuroendocrine factors that affect LH release such as gonadotropin-inhibitory hormone (Son et al., 2012).

In addition to the parameters examined in the present study, it is likely that other synaptic and intrinsic properties of GnRH neurons change with cycle stage. With regard to the former, estradiol suppresses glutamatergic excitatory fast synaptic transmission during negative feedback in the daily surge model (Christian et al., 2009), and increased glutamatergic transmission on proestrus in rats (Tada et al., 2013). In another estrogen-induced surge model, the density of spines, often considered a termina-
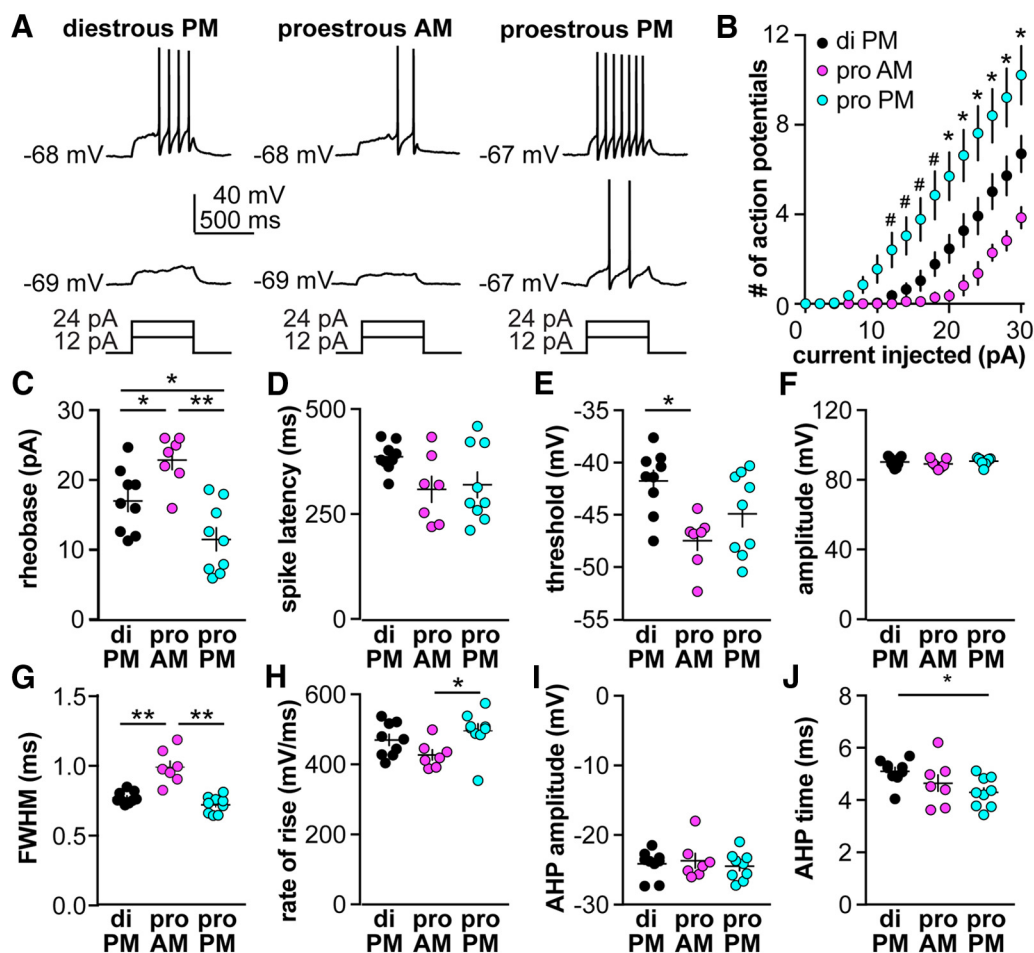
Figure 3. GnRH neuron excitability is increased on proestrus versus diestrus. *A*, Representative traces from a neuron in each group during 500-ms current injections of 12 and 24 pA (current injection protocol below). *B*, Mean ± SEM spikes elicited for each current injection step (two-way repeated-measures ANOVA cycle stage: $F_{(2,22)} = 10.2$, current: $F_{(15,330)} = 93.03$, interaction: $F_{(30,330)} = 9.503$, $*p < 0.05$ diestrous PM vs proestrous PM and $p < 0.05$ proestrous AM vs proestrous PM; $*p < 0.05$ among all three groups, Fisher's LSD). *C–H*, Individual values and mean ± SEM for: (*C*) rheobase current (ANOVA $F_{(2,22)} = 12.8$, $*p < 0.05$, $**p < 0.0001$), (*D*) latency to first spike (ANOVA $F_{(2,22)} = 2.85$, $p = 0.0792$), (*E*) action potential threshold (ANOVA $F_{(2,22)} = 6.18$, $*p < 0.01$ Tukey), (*F*) action potential amplitude (ANOVA, $F_{(2,22)} = 0.676$), (*G*) FWHM (ANOVA $F_{(2,22)} = 26.2$, $**p < 0.0001$ Tukey), (*H*) action potential rate of rise (Kruskal–Wallis, KW = 6.69, $*p < 0.05$ Dunn's), (*I*) AHP amplitude (ANOVA $F_{(2,22)} = 0.252$), and (*J*) AHP time (Kruskal–Wallis, KW = 7.03, $*p < 0.05$ Dunn's).

tion point for glutamatergic inputs, was increased in GnRH neurons expressing cFos as a marker of elevated neuronal activity during the surge (Chan et al., 2011). With regard to intrinsic properties, a decrease in both transient A-type and sustained delayed rectifier potassium currents (DeFazio and Moenter, 2002; Pielecka-Fortuna et al., 2011) and an increase in both low and high-voltage activated calcium currents have been reported during positive feedback using different estradiol regimens (Zhang et al., 2009; Sun et al., 2010). Similar changes in specific voltage-gated ion channels may underlie the changes in excitability observed among cycle stages in the present study. Of note, the lower excitability of cells recorded on the morning of proestrus and lower Rin compared to either the afternoon of diestrus or negative feedback (OVX+E AM) in the daily surge model may suggest greater changes in these and perhaps other conductances occur during the morning of proestrus (Adams et al., 2018).

The concept that estradiol regulates synaptic properties of GnRH neurons to bring about the switch from negative to positive feedback were not supported in recent work using another LH-surge induction model in which OVX mice are treated with basal estradiol replacement then an additional estrogen injection to mimic the proestrous estradiol rise (Bronson and Vom Saal, 1979b; Bronson, 1981). No differences were observed in sPSC or mPSC frequency between negative feedback (OVX+basal E, slices made 4.5–5 h before lights out, recordings made 1–3.5 h before lights off) and positive feedback (OVX+ basal E + E injection, slices made 1.5–2 h before lights out, recordings 1 h before to 1.5 h after lights out; Liu et al., 2017). Despite this difference, both models reliably produce an LH surge. This could indicate that changes in GABAergic PSC frequency may not be necessary for initiating positive feedback but may mark cotransmission of other substances such as kisspeptin (Lee et al., 2010; Piet et al., 2018). In this regard, knockout of estradiol

receptor α from GABAergic neurons eliminates estradiol positive feedback (Cheong et al., 2015). Of note, this would remove ERα from a large percentage of kisspeptin neurons in the anteroventral periventricular region that use GABA as a co-transmitter; the lack of a surge may reflect reduced activation of these neurons (Cravo et al., 2011; Frazao et al., 2013). Another possibility is that the overlap of recording time relative to lights out in the former study precluded detection of a difference between negative and positive feedback. If time of day interacts with estradiol to generate the changes observed in synaptic transmission to GnRH neurons, as suggested by the present data comparing proestrous AM and PM and previous work in the daily surge model, it is possible that the switch to positive feedback levels of transmission had already occurred based on basal estradiol alone. Of note, the frequency of synaptic transmission in that study is higher in all groups that we have observed either in daily surge or cycling mice.

The LH surge is critical for ovulation, reproduction and the continuation of species. The present studies add to a literature that indicates multiple factors can influence the switch from negative to positive feedback, and further indicates that the mechanisms producing negative feedback are also changing throughout the cycle. Feedback stage-dependent shifts in both GnRH neuron intrinsic excitability and fast-synaptic inputs likely contribute to the increase in firing rate and GnRH release during positive feedback.

References

Adams C, Stroberg W, DeFazio RA, Schnell S, Moenter SM (2018) Gonadotropin-releasing hormone (GnRH) neuron excitability is regulated by estradiol feedback and kisspeptin. J Neurosci 38: 1249–1263. CrossRef Medline

Auger C, Marty A (2000) Quantal currents at single-site central synapses. J Physiol 526:3–11. Medline

Barrell GK, Moenter SM, Caraty A, Karsch FJ (1992) Seasonal changes of gonadotropin-releasing hormone secretion in the ewe. Biol Reprod 46:1130–1135. Medline

Barry PH (1994) JPCalc, a software package for calculating liquid junction potential corrections in patch-clamp, intracellular, epithelial and bilayer measurements and for correcting junction potential measurements. J Neurosci Methods 51:107–116. Medline

Bronson FH (1981) The regulation of luteinizing hormone secretion by estrogen: relationships among negative feedback, surge potential, and male stimulation in juvenile, peripubertal, and adult female mice. Endocrinology 108:506–516. CrossRef Medline

Bronson FH, Vom Saal FS (1979a) Control of the preovulatory release of luteinizing hormone by steroids in the mouse. Endocrinology 104:1247–1255. CrossRef Medline

Bronson FH, Vom Saal FS (1979b) Control of the preovulatory release of luteinizing hormone by steroids in the mouse. Endocrinology 104:1247–1255. CrossRef

Chan H, Prescott M, Ong Z, Herde MK, Herbison AE, Campbell RE (2011) Dendritic spine plasticity in gonadatropin-releasing hormone (GnRH) neurons activated at the time of the preovulatory surge. Endocrinology 152:4906–4914. CrossRef Medline

Chappell PE, Levine JE (2000) Stimulation of gonadotropin-releasing hormone surges by estrogen. I. Role of hypothalamic progesterone receptors. Endocrinology 141:1477–1485. CrossRef Medline

Chappell PE, Schneider JS, Kim P, Xu M, Lydon JP, O'Malley BW, Levine JE (1999) Absence of gonadotropin surges and gonadotropin-releasing hormone self-priming in ovariectomized (OVX), estrogen (E2)-treated, progesterone receptor knockout (PRKO) mice. Endocrinology 140:3653–3658. CrossRef Medline

Cheong RY, Czieselsky K, Porteous R, Herbison AE (2015) Expression of ESR1 in glutamatergic and GABAergic neurons is essential for normal puberty onset, estrogen feedback, and fertility in female mice. J Neurosci 35:14533–14543. CrossRef Medline

Christian CA, Moenter SM (2007) Estradiol induces diurnal shifts in GABA transmission to gonadotropin-releasing hormone neurons to provide a neural signal for ovulation. J Neurosci 27:1913–1921. CrossRef Medline

Christian CA, Mobley JL, Moenter SM (2005) Diurnal and estradiol-dependent changes in gonadotropin-releasing hormone neuron firing activity. Proc Natl Acad Sci USA 102:15682–15687. CrossRef Medline

Christian CA, Pielecka-Fortuna J, Moenter SM (2009) Estradiol suppresses glutamatergic transmission to gonadotropin-releasing hormone neurons in a model of negative feedback in mice. Biol Reprod 80:1128–1135. CrossRef

Cravo RM, Margatho LO, Osborne-Lawrence S, Donato J Jr, Atkin S, Bookout AL, Rovinsky S, Frazão R, Lee CE, Gautron L, Zigman JM, Elias CF (2011) Characterization of Kiss1 neurons using transgenic mouse models. Neuroscience 173:37–56. CrossRef

Czieselsky K, Prescott M, Porteous R, Campos P, Clarkson J, Steyn FJ, Campbell RE, Herbison AE (2016) Pulse and surge profiles of luteinizing hormone secretion in the mouse. Endocrinology 157: 4794–4802. CrossRef Medline

DeFazio RA, Moenter SM (2002) Estradiol feedback alters potassium currents and firing properties of gonadotropin-releasing hormone neurons. Mol Endocrinol 16:2255–2265. CrossRef Medline

DeFazio RA, Elias CF, Moenter SM (2014) GABAergic transmission to kisspeptin neurons is differentially regulated by time of day and estradiol in female mice. J Neurosci 34:16296–16308. CrossRef Medline

Docke F, Dorner G (1965) The mechanism of the induction of ovulation by oestrogens. J Endocrinol 33:491–499.

Evans NP, Dahl GE, Padmanabhan V, Thrun LA, Karsch FJ (1997) Estradiol requirements for induction and maintenance of the gonadotropin-releasing hormone surge: implications for neuroendocrine processing of the estradiol signal. Endocrinology 138: 5408–5414. CrossRef Medline

Everett JW, Sawyer CH (1950) A 24-hour periodicity in the "LH-release apparatus" of female rats, disclosed by barbiturate sedation. Endocrinology 47:198–218. CrossRef Medline

Frazao R, Cravo RM, Donato J Jr, Ratra DV, Clegg DJ, Elmquist JK, Zigman JM, Williams KW, Elias CF (2013) Shift in Kiss1 cell activity requires estrogen receptor α. J Neurosci 33:2807–2820. CrossRef

Hutchens EG, Ramsey KA, Howard LC, Abshire MY, Patrie JT, McCartney CR (2016) Progesterone has rapid positive feedback actions on LH release but fails to reduce LH pulse frequency within 12 h in estradiol-pretreated women. Physiol Rep 4.

Kaeser PS, Regehr WG (2014) Molecular mechanisms for synchronous, asynchronous, and spontaneous neurotransmitter release. Annu Rev Physiol 76:333–363. CrossRef Medline

Karsch FJ, Cummins JT, Thomas GB, Clarke IJ (1987) Steroid feedback inhibition of pulsatile secretion of gonadotropin-releasing hormone in the ewe. Biol Reprod 36:1207–1218. CrossRef Medline

Lee K, Porteous R, Campbell RE, Lüscher B, Herbison AE (2010) Knockdown of GABA(A) receptor signaling in GnRH neurons has minimal effects upon fertility. Endocrinology 151:4428–4436. CrossRef

Legan SJ, Karsch FJ (1975) A daily signal for the LH surge in the rat. Endocrinology 96:57–62. CrossRef Medline

Levine JE, Ramirez VD (1982) Luteinizing hormone-releasing hormone release during the rat estrous cycle and after ovariectomy, as estimated with push-pull cannulae. Endocrinology 111:1439–1448. CrossRef Medline

Liu X, Porteous R, Herbison AE (2017) Dynamics of GnRH neuron ionotropic GABA and glutamate synaptic receptors are unchanged during estrogen positive and negative feedback in female mice. eNeuro 4.

Micevych P, Sinchak K (2011) The neurosteroid progesterone underlies estrogen positive feedback of the LH surge. Front Endocrinol (Lausanne) 2:90. CrossRef Medline

Moenter SM, Caraty A, Karsch FJ (1990) The estradiol-induced surge of gonadotropin-releasing hormone in the ewe. Endocrinology 127:1375–1384. CrossRef Medline

Moenter SM, Caraty A, Locatelli A, Karsch FJ (1991) Pattern of gonadotropin-releasing hormone (GnRH) secretion leading up to ovulation in the ewe: existence of a preovulatory GnRH surge. Endocrinology 129:1175–1182. CrossRef Medline

Norman RL, Blake CA, Sawyer CH (1973) Estrogen-dependent 24-hour periodicity in pituitary LH release in the female hamster. Endocrinology 93:965–970. CrossRef Medline

Pielecka J, Quaynor SD, Moenter SM (2006) Androgens increase gonadotropin-releasing hormone neuron firing activity in females and interfere with progesterone negative feedback. Endocrinology 147:1474–1479. CrossRef Medline

Pielecka-Fortuna J, DeFazio RA, Moenter SM (2011) Voltage-gated potassium currents are targets of diurnal changes in estradiol feedback regulation and kisspeptin action on gonadotropin-releasing hormone neurons in mice. Biol Reprod 85:987–995. CrossRef Medline

Piet R, Kalil B, McLennan T, Porteous R, Czieselsky K, Herbison AE (2018) Dominant neuropeptide cotransmission in kisspeptin-GABA regulation of GnRH neuron firing driving ovulation. J Neurosci 38:6310–6322. CrossRef

Sarkar DK, Chiappa SA, Fink G, Sherwood NM (1976) Gonadotropin-releasing hormone surge in pro-oestrous rats. Nature 264:461–463. Medline

Schally AV, Arimura A, Kastin AJ, Matsuo H, Baba Y, Redding TW, Nair RM, Debeljuk L, White WF (1971) Gonadotropin-releasing hormone: one polypeptide regulates secretion of luteinizing and follicle-stimulating hormones. Science 173:1036–1038. Medline

Shim WS, Conaway M, Masamura S, Yue W, Wang JP, Kmar R, Santen RJ (2000) Estradiol hypersensitivity and mitogen-activated protein kinase expression in long-term estrogen deprived human breast cancer cells in vivo. Endocrinology 141:396–405. CrossRef Medline

Silveira M, Burger LL, DeFazio RA, Wagenmaker ER, Moenter SM (2017) GnRH neuron activity and pituitary response in estradiol-induced vs proestrous luteinizing hormone surges in female mice. Endocrinology 158:356–366.

Son YL, Ubuka T, Millar RP, Kanasaki H, Tsutsui K (2012) Gonadotropin-inhibitory hormone inhibits GnRH-induced gonadotropin subunit gene transcriptions by inhibiting AC/cAMP/PKA-dependent ERK pathway in LβT2 cells. Endocrinology 153:2332–2343. CrossRef Medline

Sun J, Chu Z, Moenter SM (2010) Diurnal in vivo and rapid in vitro effects of estradiol on voltage-gated calcium channels in gonadotropin-releasing hormone neurons. J Neurosci 30:3912–3923. CrossRef Medline

Suter KJ, Song WJ, Sampson TL, Wuarin JP, Saunders JT, Dudek FE, Moenter SM (2000) Genetic targeting of green fluorescent protein to gonadotropin-releasing hormone neurons: characterization of whole-cell electrophysiological properties and morphology. Endocrinology 141:412–419. CrossRef Medline

Tada H, Kuroki Y, Funabashi T, Kamiya Y, Goto T, Suyama K, Sano A, Mitsushima D, Etgen AM, Takahashi T (2013) Phasic synaptic incorporation of GluR2-lacking AMPA receptors at gonadotropin-releasing hormone neurons is involved in the generation of the luteinizing hormone surge in female rats. Neuroscience 248:664–669. CrossRef Medline

Zhang C, Bosch MA, Rick EA, Kelly MJ, Rønnekleiv OK (2009) 17Beta-estradiol regulation of T-type calcium channels in gonadotropin-releasing hormone neurons. J Neurosci 29:10552–10562. CrossRef Medline